

## Micro-sphere layered targets efficiency in laser driven proton acceleration

V. Floquet,<sup>1</sup> O. Klimo,<sup>2</sup> J. Psikal,<sup>2</sup> A. Velyhan,<sup>3</sup> J. Limpouch,<sup>2</sup> J. Proška,<sup>2</sup> F. Novotny,<sup>2</sup> L. Stolcova,<sup>2</sup> A. Macchi,<sup>4,5</sup> A. Sgattoni,<sup>4,6</sup> L. Vassura,<sup>7,8</sup> L. Labate,<sup>4</sup> F. Baffigi,<sup>4</sup> L. A. Gizzi,<sup>4</sup> Ph. Martin,<sup>1</sup> and T. Ceccotti<sup>1,a)</sup>

<sup>1</sup>CEA, IRAMIS, SPAM, F-91191 Gif-sur-Yvette, France

<sup>2</sup>FNSPE, Czech Technical University in Prague, CR-11519 Prague, Czech Republic

<sup>3</sup>Institute of Physics v.v.i. ASCR, Na Slovance 1999, Prague, Czech Republic

<sup>4</sup>Istituto Nazionale di Ottica, Consiglio Nazionale delle Ricerche, research unit “Adriano Gozzini,” Via G. Moruzzi 1, 56124 Pisa, Italy

<sup>5</sup>Dipartimento di Fisica “Enrico Fermi,” Università di Pisa, largo Bruno Pontecorvo 3, 56127 Pisa, Italy

<sup>6</sup>Dipartimento di Energia, Politecnico di Milano, Milano, Italy

<sup>7</sup>LULI, UMR7605, CNRS-CEA-Ecole Polytechnique-Paris 6, 91128 Palaiseau, France

<sup>8</sup>Dipartimento SBAI, Università di Roma “La Sapienza,” Via A. Scarpa 14, 00161 Roma, Italy

(Received 12 July 2013; accepted 9 August 2013; published online 28 August 2013)

Proton acceleration from the interaction of high contrast, 25 fs laser pulses at  $>10^{19}$  W/cm<sup>2</sup> intensity with plastic foils covered with a single layer of regularly packed micro-spheres has been investigated experimentally. The proton cut-off energy has been measured as a function of the micro-sphere size and laser incidence angle for different substrate thickness, and for both *P* and *S* polarization. The presence of micro-spheres with a size comparable to the laser wavelength allows to increase the proton cut-off energy for both polarizations at small angles of incidence (10°). For large angles of incidence, however, proton energy enhancement with respect to flat targets is absent. Analysis of electron trajectories in particle-in-cell simulations highlights the role of the surface geometry in the heating of electrons. © 2013 AIP Publishing LLC. [<http://dx.doi.org/10.1063/1.4819239>]

### I. INTRODUCTION

Acceleration of ions with high intensity laser pulses has been raising great interest for more than twelve years<sup>1</sup> and we nowadays have a detailed knowledge of the main acceleration mechanism, known as Target Normal Sheath Acceleration (TNSA). During the interaction of a high intensity laser pulse with a solid target (usually a micrometric thick foil), a fraction of the laser energy is transferred to a population of hot electrons. These latter migrate through the target and cross the rear target/vacuum interface, producing a sheath electric field of the order of some TV/m which accelerates ions (mainly protons due to their favorable mass/charge ratio). The characterization of proton emission provides a diagnostic for the processes of laser energy absorption and fast electron generation and transport in solid targets.<sup>2</sup> The energy, duration, flow, divergence, and laminarity characteristics of TNSA-accelerated ions allow to use them for several application such as isochoric heating,<sup>3</sup> ultrafast probing of electromagnetic fields in plasmas,<sup>4</sup> radiography of dense matter,<sup>5</sup> and radiobiological studies.<sup>6</sup> In addition, there is potential for laser-driven nuclear physics applications such as neutron production<sup>7</sup> and isotope production for positron emission tomography,<sup>8</sup> especially if ion acceleration can be optimized for femtosecond, small-scale laser systems.

With particular regard to the latter applications (and focusing on the acceleration of protons in the following), it is important to investigate strategies to enhance both the proton maximum energy and the laser energy conversion efficiency,

and possibly to tailor their spectral distribution. One of the suggested ways is using structured targets in order to increase the coupling efficiency. Examples of such targets, having either nanometric<sup>9</sup> or micrometric<sup>10</sup> structures on the irradiated surface, have been already investigated. The observed X-ray yield enhancement<sup>11</sup> has been ascribed, for instance, to the action of multipass stochastic heating of the hot electrons in the oscillating laser field.<sup>12</sup>

This paper reports on an experimental study of “Micro-Spheres Targets” (MSTs) composed by a thin ( $\sim\mu\text{m}$  thick) plastic foil (substrate) with a mono-layer of hexagonally packed micrometer polystyrene spheres on its surface. The work here reported follows from previous indications by particle-in-cell simulations of MST targets,<sup>13</sup> showing enhancement of absorption and proton energy, and is complementary to similar measurements on a different laser system.<sup>14,15</sup> We studied the influence of laser polarization and incidence angle as well as of the structure size on the coupling efficiency of MSTs on the proton cut-off energies.

### II. EXPERIMENTAL SET-UP AND TARGET STRUCTURE

The experiment was performed on the UHI-100 laser facility at CEA-Saclay. UHI-100 is a Ti:Sa laser delivering up to 2 J in a 25 fs pulse, with a contrast ratio better than  $10^8$  which is further improved to about  $10^{12}$  using a double plasma mirror (DPM).<sup>16</sup> This latter feature is essential in order to preserve the MST surface structures. Laser wavefront correction is accomplished through a deformable mirror which enables to focus the laser pulse down to a  $6\mu\text{m}$  (FWHM) spot by using an *f*/3.75 off-axis parabola. The laser energy measured after the pulse compressor and the plasma

<sup>a)</sup>tiberio.ceccotti@cea.fr

mirror was 0.79 J, and after the focusing optics a 50% of such energy inside a  $1/e^2$  spot was estimated. This corresponds to 0.2 J in the FWHM spot, leading to a peak intensity of  $I = 2.8 \times 10^{19} \text{ W cm}^{-2}$ . A rotating  $\lambda/2$  wave plate was put on the laser path in order to study the influence of the pulse polarization ( $P$  or  $S$ ). The incidence angle was varied from  $10^\circ$  up to  $45^\circ$  turning the target holder (around its vertical axis) without modifying the laser optical path. Proton emission was measured by a Thomson parabola, detecting proton energies ranging from 400 keV to 20 MeV (with a resolution  $\Delta E/E \approx 5 \times 10^{-2}$  for the highest energies).

Targets were made of a thick Mylar substrate with different thicknesses (900 nm, 20  $\mu\text{m}$ , and 40  $\mu\text{m}$ ) and a single layer of either 471 nm or 940 nm diameter polystyrene micro-spheres deposited at the surface in a hexagonal layout (see Fig. 1).

### III. EXPERIMENTAL RESULTS

In Fig. 2, we show the measured cut-off proton energies as a function of the micro-sphere size for  $P$  polarized laser pulses at  $10^\circ$  incident angle. The 0  $\mu\text{m}$  sphere size refers to simple foils without any structured layer. As expected on the basis of previous investigations with the same laser system, we did not detect any proton emission using 20 and 40  $\mu\text{m}$  simple foils, due to their considerable thickness and to the small incidence angle. Nevertheless, repeating the measurements using 20 and 40  $\mu\text{m}$  substrate MSTs, we observed that the presence of structures, and in particular of the 940 nm diameter micro-spheres, increases the proton energies above the detection threshold. Measurements in  $S$  polarization are reported too showing that the surface modulation induced by the spheres layer allows to transfer the laser energy to the target as effectively as in  $P$  polarization.

The observations are in qualitative agreement both with simulation results<sup>13</sup> and with independent experimental measurements.<sup>14</sup> With respect to the latter, quantitative differences in the energy values and in the “optimal” size of the spheres may be ascribed to different parameters, including target thickness, laser intensity and incidence angle. Taking the detection threshold as an upper limit for the proton

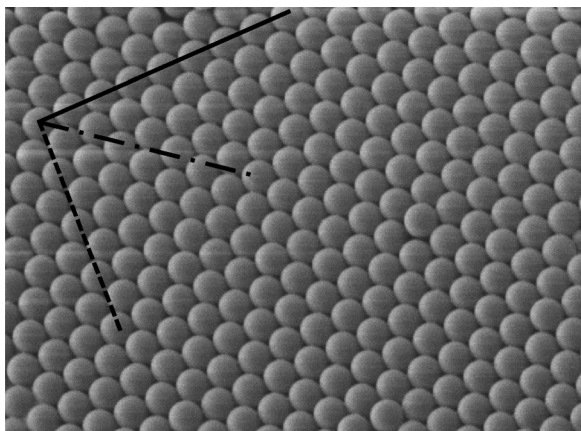


FIG. 1. Scanning Electron Microscopy picture of the 940 nm micro-sphere hexagonal layout of a MST. The lines indicate three different directions along which the structure would present a different spatial period.

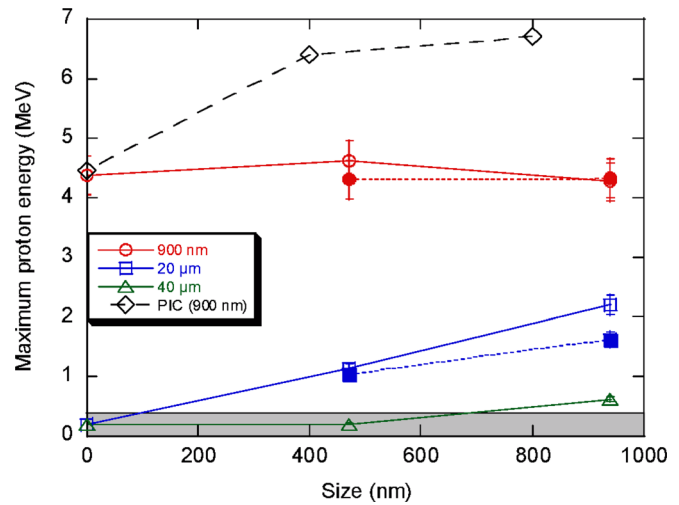


FIG. 2. Proton maximum energies as a function of micro-sphere size for different substrate thickness and PIC simulation data for a 900 nm substrate.  $P$  and  $S$  polarization measurements are reported as empty and filled marks respectively. Here and in Fig. 3, each point (error bar) represents the average value (statistical error) of five consecutive laser shots. Measurements falling under the diagnostic detection threshold (gray filled region in the plot) have been reported as an arbitrary 0.2 MeV constant value (for plot clarity sake, low energy  $S$  data have been omitted).

cut-off energy in flat targets, the relative enhancement in the case of 470 nm spheres is at least a factor of 2.5 and may further double for the 940 nm sphere, as shown in Fig. 2. Such enhancement factor is larger than observed in Ref. 14 at higher intensity. Furthermore, recent additional measurements<sup>15</sup> on the same laser system of Ref. 14 showed that both the relative increase with respect to flat targets and the dependence on the sphere’s thickness become much smoother at higher intensity.

On the other hand, the 900 nm thick MSTs show energy values close to those observed for the simple foils, in contrast with 2D Particle-In-Cell (PIC) simulation results (see Ref. 13 for details), which foresee a cut-off energy enhancement of about 50% for both sphere sizes. Notice that the PIC simulations for flat thin targets reproduce well the observed energy cut-off, which is much higher than for thicker targets due to the contribution of electron recirculation process<sup>17</sup> (under our interaction conditions recirculation should enhance the proton energy for thicknesses approximately in the 500 nm–2  $\mu\text{m}$  range<sup>18</sup>). The strong discrepancy between experiment and simulation for the layered sphere case should then be ascribed to some technical or manufacturing issue with very thin foils, of thickness comparable to the diameter of the spheres, such as insufficient adhesion to the surface or wrapping and deformation of the foil. The exact nature of the failure to yield enhanced acceleration in the thinnest target case is not fully clear at present. In Ref. 14, the energy enhancement was observed for 1  $\mu\text{m}$  thickness but with significant fluctuations, which supports the possibility of technical issues with thin targets.

Figure 3 reports the variation of proton energy as a function of the incidence angle, for  $P$  and  $S$  polarized laser pulses and the 20  $\mu\text{m}$  thick, 940 nm spheres MST. While both  $P$  and  $S$  polarization give similar cut-off energies and a strong enhancement of proton energy with respect to flat targets at

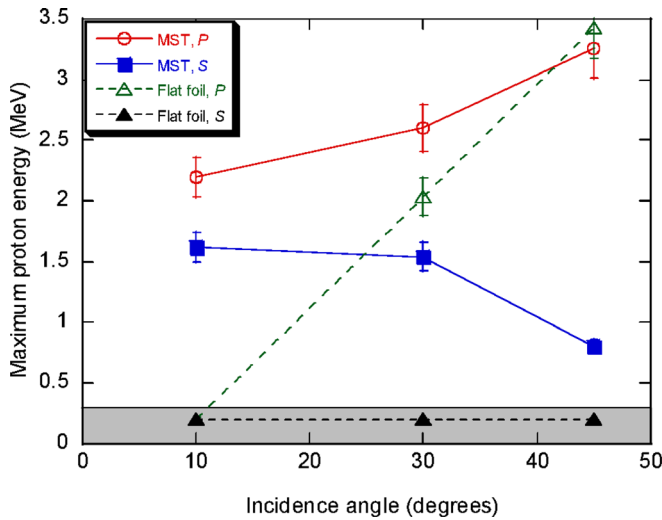


FIG. 3. Proton maximum energies as a function of the incidence angle for the 20  $\mu\text{m}$  thick MST and a 20  $\mu\text{m}$  flat Mylar foil, in  $P$  and  $S$  polarization.

the smallest angle ( $10^\circ$ ), for the largest angle ( $45^\circ$ ) the behavior is very close to flat foils, with almost the same cut-off energy for  $P$  polarization and a much lower value for  $S$  polarization. This trend may be related to the increase of both the focal spot size and the geometrical shadow effect by the structured surface for increasing angles, so that the coupling with the spheres is reduced and the interaction conditions get eventually similar to those of a flat foil.

While a comparison with Ref. 14 is not possible since in that experiment a single angle of incidence ( $22.5^\circ$ ) was investigated, the decrease of proton energy enhancement as a function of the incidence angle using  $P$  polarized laser beam agrees qualitatively with absorption measurements using targets with surface roughness of similar size.<sup>19</sup> The femtosecond laser pulse absorption (which is connected with the efficiency of ion acceleration) reported in Ref. 19 was almost constant in the range between  $20^\circ$  and  $60^\circ$  for rough surfaced targets, whereas the absorption was increasing for flat targets. The latter may be simply attributed to “vacuum heating” (or Brunel effect),<sup>20</sup> which is driven by the electric field component of the laser field and is more efficient at large incidence angles. The absence of protons with energy above the cut-off threshold observed in the case of  $S$  polarization and flat targets suggests that the role of relativistic  $J \times B$  heating<sup>21</sup> is negligible in the investigated regime of laser intensity and plasma density.

#### IV. SIMULATION RESULTS

To go deeper into the interpretation of the increased absorption due to the spheres layer, the trajectories of individual particles in PIC simulations (similar to those reported in Ref. 13) have been studied. Specifically, we analyzed the trajectories of 9000 electrons in 2D PIC simulations with a dimensionless peak amplitude  $a_0 = 1.5$  and density  $n_e = 40n_c$  (corresponding to an intensity of  $4.9 \times 10^{18} \text{ W cm}^{-2}$  and  $n_e = 6.9 \times 10^{22} \text{ cm}^{-3}$  for  $\lambda = 0.8 \mu\text{m}$ ). The simulation considered a plane laser wave and stationary ions. According

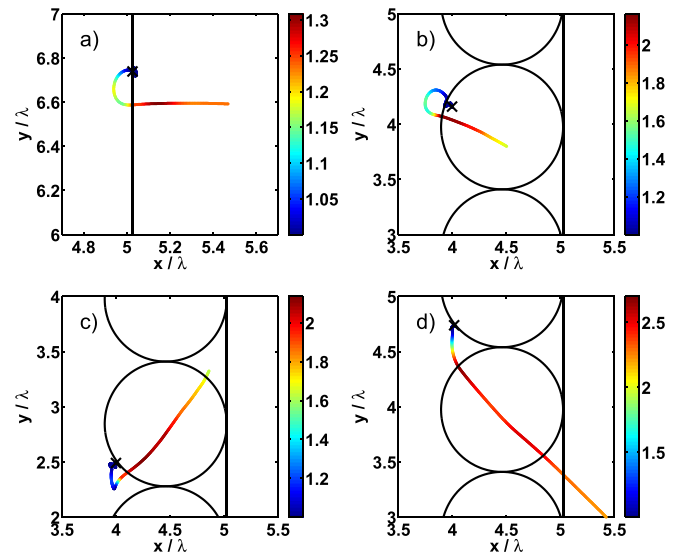


FIG. 4. 2D PIC simulations of electron trajectories for normal incidence ( $a_0 = 1.5$ ) and stationary ions. Color represents the relativistic gamma factor of electrons. We considered a flat foil (a) and a MST with electrons traveling from the front part of the sphere and going back into the same sphere (b), or accelerated from the side part and re-entering the same sphere (c) or the neighboring one (d).

to this analysis, we can distinguish three main components of the population of electrons which are accelerated in MSTs. The first one includes electrons that originate from the “top” of the spheres (see Fig. 4(b)) and release the energy they gain in the same sphere (releasing of energy is identified with re-entering the target at high velocity, as in the simple picture of the Brunel effect<sup>20</sup>). Another fraction of accelerated electrons comes from the side surface of spheres and re-enter into the same sphere too (Fig. 4(c)). These two processes are quite close to the corresponding mechanism observed in a flat foil at normal and oblique incidence respectively and gather about 40% of the overall electron population. However, the observed absorption increase is mainly due to the electrons accelerated from the side of the spheres which deposit their energy in the very neighboring sphere in half a laser period (Fig. 4(d)). Indeed, these last electrons may deposit their energy after getting the maximum acceleration and before being decelerated by the second half laser period. As a consequence, if the distance between two spheres is either too large or too small, this process shows a lower efficiency. This analysis of electron trajectory may help to explain the stochastic heating which takes place in the closely packed configuration of microspheres but it does not exclude other efficient laser absorption mechanisms with different electron trajectories if the separation distance between spheres is larger.

It may be noticed that MSTs are represented in 2D simulations as an array of adjacent, closely packed wires (3D spheres become wires in 2D due to the translational invariance in the direction normal to the simulation plane) with a fixed distance between the centers and tips of all the spheres (in other words the 2D system has a discrete translational symmetry, with a period equal to the sphere/wire diameter). Nonetheless, in a real target with an hexagonal MST layout, the electrons traveling on a line parallel to the surface would see a spatial periodicity equal to the size of the sphere only

along a limited set of directions (the three axes of symmetry passing through the midpoints of opposite sides and the center of the hexagonal lattice; see Fig. 1). According to their initial acceleration direction, electrons can cross a vacuum region between any couple of spheres or take a path showing an even more complicated periodicity of the system (dotted and dashed-dotted lines respectively in Fig. 1). Thus, multi-pass stochastic heating may behave differently in a real 3D geometry (not computationally accessible at present) and the acceleration dynamics may depend upon the angle between the laser polarization and the lattice symmetry axis, which is not controlled in the experiment.

## V. CONCLUSIONS

In conclusion, an enhancement of the proton energy cutoff has been observed in thick plastic targets covered with a layer of microspheres, in broad agreement with previous simulation results and independent measurements. However, it has also been shown that the enhancement is not effective at large incidence angles for thick substrates. The analysis of electron trajectories in particle-in-cell simulations have highlighted their role in leading to absorption in a pattern of regularly packed sphere.

## ACKNOWLEDGMENTS

The research leading to these results has received funding from LASERLAB-EUROPE (Grant Agreement No. 284464, EU's Seventh Framework Programme), proposal n.SLIC001693. We acknowledge the ANR Blanc (GOSPEL, project BLAN08-1 380251), the Triangle of Physics (APPEAL), the Labex PALM, EGIDE, the Ile-de-France region (SESAME), the SAPHIR consortium (OSEO) and the regional board of Essonne (ASTRE) for their financial support. Partial support by the Czech Science Foundation (Project P205/11/1165), by the MSMT ECOP project (CZ.1.07/2.3.00/20.0087), and by MIUR (Italy) via the FIR project "SULDIS" are also acknowledged.

<sup>1</sup>M. Borghesi, J. Fuchs, S. V. Bulanov, A. J. MacKinnon, P. K. Patel, and M. Roth, *Fusion Sci. Technol.* **49**, 412 (2006); available at [http://www.ans.org/pubs/journals/fst/a\\_1159](http://www.ans.org/pubs/journals/fst/a_1159). H. Daido, M. Nishiuchi, and A. S. Pirozhkov, *Rep. Prog. Phys.* **75**, 056401 (2012); A. Macchi, M. Borghesi, and M. Passoni, *Rev. Mod. Phys.* **85**, 751 (2013).

<sup>2</sup>J. Fuchs, T. E. Cowan, P. Audebert, H. Ruhl, L. Gremillet, A. Kemp, M. Allen, A. Blazevic, J.-C. Gauthier, M. Geissel, M. Hegelich, S. Karsch, P. Parks, M. Roth, Y. Sentoku, R. Stephens, and E. M. Campbell, *Phys. Rev. Lett.* **91**, 255002 (2003); M. Kaluza, J. Schreiber, M. I. K. Santala, G. D. Tsakiris, K. Eidmann, J. Meyer-ter Vehn, and K. J. Witte, *Phys. Rev. Lett.* **93**, 045003 (2004); P. McKenna, D. C. Carroll, R. J. Clarke, R. G. Evans, K. W. D. Ledingham, F. Lindau, O. Lundh, T. McCanny, D. Neely, A. P. L. Robinson, L. Robson, P. T. Simpson, C.-G. Wahlström, and M. Zepf, *Phys. Rev. Lett.* **98**, 145001 (2007); P. McKenna, A. P. L. Robinson, D. Neely, M. P. Desjarlais, D. C. Carroll, M. N. Quinn, X. H. Yuan, C. M. Brenner, M. Burza, M. Coury, P. Gallegos, R. J. Gray, K. L. Lancaster, Y. T. Li, X. X. Lin, O. Tresca, and C.-G. Wahlström, *Phys. Rev. Lett.* **106**, 185004 (2011).

<sup>3</sup>P. K. Patel, A. J. Mackinnon, M. H. Key, T. E. Cowan, M. E. Ford, M. Allen, D. F. Price, H. Ruhl, P. T. Springer, and R. Stephens, *Phys. Rev. Lett.* **91**, 125004 (2003); A. Mancic, J. Robiche, P. Antici, P. Audebert, C. Blancard, P. Combis, F. Dorchies, G. Faussurier, S. Fourmaux, M. Harmand, R. Kodama, L. Lancia, S. Mazevet, M. Nakatsutsumi, O.

Peyrusse, V. Recoules, P. Renaudin, R. Shepherd, and J. Fuchs, *High Energy Density Phys.* **6**, 21 (2010).

<sup>4</sup>M. Borghesi, L. Romagnani, A. Schiavi, D. H. Campbell, M. G. Haines, O. Willi, A. J. Mackinnon, M. Galimberti, L. Gizzi, R. J. Clarke, and S. Hawkes, *Appl. Phys. Lett.* **82**, 1529 (2003); A. J. Mackinnon, P. K. Patel, D. W. Price, D. Hicks, L. Romagnani, and M. Borghesi, *Appl. Phys. Lett.* **82**, 3188 (2003); N. L. Kugland, D. D. Ryutov, C. Plechaty, J. S. Ross, and H.-S. Park, *Rev. Sci. Instrum.* **83**, 101301 (2012).

<sup>5</sup>A. J. Mackinnon, P. K. Patel, M. Borghesi, R. C. Clarke, R. R. Freeman, H. Habara, S. P. Hatchett, D. Hey, D. G. Hicks, S. Kar, M. H. Key, J. A. King, K. Lancaster, D. Neely, A. Nikkro, P. A. Norreys, M. M. Notley, T. W. Phillips, L. Romagnani, R. A. Snavely, R. B. Stephens, and R. P. J. Town, *Phys. Rev. Lett.* **97**, 045001 (2006); A. B. Zylstra, C. K. Li, H. G. Rinderknecht, F. H. Séguin, R. D. Petrasso, C. Stoeckl, D. D. Meyerhofer, P. Nilson, T. C. Sangster, S. L. Pape, A. Mackinnon, and P. Patel, *Rev. Sci. Instrum.* **83**, 013511 (2012).

<sup>6</sup>A. Yogo, K. Sato, M. Nishikino, M. Mori, T. Teshima, H. Numasaki, M. Murakami, Y. Demizu, S. Akagi, S. Nagayama, K. Ogura, A. Sagisaka, S. Orimo, M. Nishiuchi, A. S. Pirozhkov, M. Ikegami, M. Tampon, H. Sakaki, M. Suzuki, I. Daito, Y. Oishi, H. Sugiyama, H. Kiriyama, H. Okada, S. Kanazawa, S. Kondo, T. Shimomura, Y. Nakai, M. Tanoue, H. Sasao, D. Wakai, P. R. Bolton, and H. Daido, *Appl. Phys. Lett.* **94**, 181502 (2009); A. Yogo, T. Maeda, T. Hori, H. Sakaki, K. Ogura, M. Nishiuchi, A. Sagisaka, H. Kiriyama, H. Okada, S. Kanazawa, T. Shimomura, Y. Nakai, M. Tanoue, F. Sasao, P. R. Bolton, M. Murakami, T. Nomura, S. Kawanishi, and K. Kondo, *Appl. Phys. Lett.* **98**, 053701 (2011); S. D. Kraft, C. Richter, K. Zeil, M. Baumann, E. Beyreuther, S. Bock, M. Bussmann, T. E. Cowan, Y. Dammene, W. Enghardt, U. Helbig, L. Karsch, T. Kluge, L. Laschinsky, E. Lessmann, J. Metzkes, D. Naumburger, R. Sauerbrey, M. Schürer, M. Sobiella, J. Woithe, U. Schramm, and J. Pawelke, *New J. Phys.* **12**, 085003 (2010); F. Fiorini, D. Kirby, M. Borghesi, D. Doria, J. C. G. Jeaynes, K. F. Kakolee, S. Kar, S. Kaur, K. J. Kirby, M. J. Merchant, and S. Green, *Phys. Med. Biol.* **56**, 6969 (2011).

<sup>7</sup>J. M. Yang, P. McKenna, K. W. D. Ledingham, T. McCanny, L. Robson, S. Shimizu, R. P. Singhal, M. S. Wei, K. Krushelnick, R. J. Clarke, D. Neely, and P. A. Norreys, *J. Appl. Phys.* **96**, 6912 (2004); L. Willingale, G. M. Petrov, A. Maksimchuk, J. Davis, R. R. Freeman, A. S. Joglekar, T. Matsuoka, C. D. Murphy, V. M. Ovchinnikov, A. G. R. Thomas, L. V. Woerkom, and K. Krushelnick, *Phys. Plasmas* **18**, 083106 (2011).

<sup>8</sup>S. Fritzel, V. Malka, G. Grillon, J. P. Rousseau, F. Burgy, E. Lefebvre, E. d'Humières, P. McKenna, and K. W. D. Ledingham, *Appl. Phys. Lett.* **83**, 3039 (2003); K. W. D. Ledingham, P. McKenna, T. McCanny, S. Shimizu, J. M. Yang, L. Robson, J. Zweit, J. M. Gillies, J. Bailey, G. N. Chimon, R. J. Clarke, D. Neely, P. A. Norreys, J. L. Collier, R. P. Singhal, M. S. Wei, S. P. D. Mangles, P. Nilson, K. Krushelnick, and M. Zepf, *J. Phys. D: Appl. Phys.* **37**, 2341 (2004); M. Fujimoto, K. Matsukado, H. Takahashi, Y. Kawada, S. Ohsuka, and S. Aoshima, *Rev. Sci. Instrum.* **80**, 113301 (2009); K. Ogura, T. Shizuma, T. Hayakawa, A. Yogo, M. Nishiuchi, S. Orimo, A. Sagisaka, A. Pirozhkov, M. Mori, H. Kiriyama, S. Kanazawa, S. Kondo, Y. Nakai, T. Shimomura, M. Tanoue, A. Akutsu, T. Motomura, H. Okada, T. Kimura, Y. Oishi, T. Nayuki, T. Fujii, K. Nemoto, and H. Daido, *Appl. Phys. Express* **2**, 066001 (2009).

<sup>9</sup>S. Bagchi, P. Prem Kiran, M. K. Bhuyan, S. Bose, P. Ayyub, M. Krishnamurthy, and G. Ravindra Kumar, *Laser Part. Beams* **26**, 259 (2008).

<sup>10</sup>G. Yue Hu, A. Le Lei, J. Wei Wang, L. Gen Huang, W. Tao Wang, X. Wang, Y. Xu, B. Fei Shen, J. Sheng Liu, W. Yu, R. Xin Li, and Z. Zhan Xu, *Phys. Plasmas* **17**, 083102 (2010).

<sup>11</sup>H. A. Sumeruk, S. Kneip, D. R. Symes, I. V. Churina, A. V. Belolipetski, T. D. Donnelly, and T. Ditmire, *Phys. Rev. Lett.* **98**, 045001 (2007).

<sup>12</sup>B. N. Breizman, A. V. Arefiev, and M. V. Fomyts'kyi, *Phys. Plasmas* **12**, 056706 (2005).

<sup>13</sup>O. Klimo, J. Psikal, J. Limpouch, J. Proška, F. Novotny, T. Ceccotti, V. Floquet, and S. Kawata, *New J. Phys.* **13**, 053028 (2011).

<sup>14</sup>D. Margarone, O. Klimo, I. J. Kim, J. Prokúpek, J. Limpouch, T. M. Jeong, T. Mocek, J. Pšikal, H. T. Kim, J. Proška, K. H. Nam, L. Štolcová, I. W. Choi, S. K. Lee, J. H. Sung, T. J. Yu, and G. Korn, *Phys. Rev. Lett.* **109**, 234801 (2012).

<sup>15</sup>D. Margarone, O. Klimo, I. J. Kim, J. Prokúpek, J. Limpouch, T. M. Jeong, T. Mocek, J. Psikal, H. T. Kim, J. Proška, K. H. Nam, I. W. Choi, T. Levato, L. Štolcová, S. K. Lee, M. Krus, F. Novotny, J. H. Sung, J. Kaufman, T. J. Yu, and G. Korn, *Proc. SPIE* **8780**, 878023 (2013).

- <sup>16</sup>A. Lévy, T. Ceccotti, P. D'Oliveira, F. Réau, M. Perdrix, F. Quéré, P. Monot, M. Bougeard, H. Lagadec, P. Martin, J.-P. Geindre, and P. Audebert, *Opt. Lett.* **32**, 310 (2007).
- <sup>17</sup>Y. Sentoku, T. E. Cowan, A. Kemp, and H. Ruhl, *Phys. Plasmas* **10**, 2009 (2003); T. Ceccotti, A. Lévy, H. Popescu, F. Réau, P. D'Oliveira, P. Monot, J. P. Geindre, E. Lefebvre, and P. Martin, *Phys. Rev. Lett.* **99**, 185002 (2007).
- <sup>18</sup>V. Floquet, T. Ceccotti, S. D. Dufrenoy, G. Bonnaud, L. Gremillet, P. Monot, and P. Martin, *Phys. Plasmas* **19**, 094501 (2012).
- <sup>19</sup>M. Cerchez, M. Swantusch, M. Bemke, M. Toncian, T. Toncian, C. Röde, G. Paulus, A. Andreev, and O. Willi, "Absorption of variable contrast femtosecond laser pulses by overdense plasmas in the relativistic regime," in *ECA (Euroconference Abstracts)*, ECA Europhysics Conference Abstracts,(European Physical Society (EPS), 2010), Vol. 34A, p. 5.205.
- <sup>20</sup>F. Brunel, *Phys. Rev. Lett.* **59**, 52 (1987).
- <sup>21</sup>W. L. Kruer and K. Estabrook, *Phys. Fluids* **28**, 430 (1985).